

Open Research Online

The Open University's repository of research publications and other research outputs

Using the *aa* index over the last 14 solar cycles to characterize extreme geomagnetic activity

Journal Item

How to cite:

Chapman, S. C.; Horne, R. B. and Watkins, N. W. (2020). Using the *aa* index over the last 14 solar cycles to characterize extreme geomagnetic activity. *Geophysical Research Letters*, 47(3), article no. e2019GL086524.

For guidance on citations see [FAQs](#).

© 2020 The Authors

Version: Version of Record

Link(s) to article on publisher's website:
<http://dx.doi.org/doi:10.1029/2019gl086524>

Copyright and Moral Rights for the articles on this site are retained by the individual authors and/or other copyright owners. For more information on Open Research Online's data [policy](#) on reuse of materials please consult the policies page.

oro.open.ac.uk



RESEARCH LETTER

10.1029/2019GL086524

Using the *aa* Index Over the Last 14 Solar Cycles to Characterize Extreme Geomagnetic ActivityS. C. Chapman¹, R. B. Horne², and N. W. Watkins^{1,3,4}

¹Centre for Fusion, Space and Astrophysics, Physics Department, University of Warwick, Coventry, UK, ²British Antarctic Survey, Cambridge, UK, ³Centre for the Analysis of Time Series, London School of Economics and Political Science, London, UK, ⁴Faculty of Science, Technology, Engineering and Mathematics, Open University, Milton Keynes, UK

Key Points:

- We present a new method that parameterizes extremes of 14 solar cycles of the *aa* geomagnetic index
- We find a 4% (28%) chance of at least one great (severe) storm per year over 14 solar cycles
- A DST perturbation weaker than $-1,000$ nT Carrington storm is in the same occurrence rate distribution as other superstorms since 1868

Supporting Information:

- Supporting Information S1

Correspondence to:

S. C. Chapman,
S.C.Chapman@warwick.ac.uk

Citation:

Chapman, S. C., Horne, R. B., & Watkins, N. W. (2020). Using the *aa* index over the last 14 solar cycles to characterize extreme geomagnetic activity. *Geophysical Research Letters*, *47*, e2019GL086524. <https://doi.org/10.1029/2019GL086524>

Received 3 DEC 2019

Accepted 17 JAN 2020

Accepted article online 22 JAN 2020

Abstract Geomagnetic indices are routinely used to characterize space weather event intensity. The D_{ST} index is well resolved but is only available over five solar cycles. The *aa* index extends over 14 cycles but is highly discretized with poorly resolved extremes. We parameterize extreme *aa* activity by the annual-averaged top few percent of observed values, show that these are exponentially distributed, and they track annual D_{ST} index minima. This gives a 14-cycle average of $\sim 4\%$ chance of at least one great ($D_{ST} < -500$ nT) storm and $\sim 28\%$ chance of at least one severe ($D_{ST} < -250$ nT) storm per year. At least one $D_{ST} = -809$ [−663, −955] nT event in a given year would be a 1:151 year event. Carrington event estimate $D_{ST} \sim -850$ nT is within the same distribution as other extreme activity seen in *aa* since 1868 so that its likelihood can be deduced from that of more moderate events. Events with $D_{ST} \lesssim -1,000$ nT are in a distinct class, requiring special conditions.

Plain Language Summary Here we use measurements of disturbances in the Earth's magnetic field that go back to 1868, and we present a novel way of analyzing the data to identify the largest magnetic storms going back some 80 years longer than has been done before. As a result, we are able to state the chance of at least one superstorm occurring in a year. We find that on average there is a 4% (28%) chance of at least one great (severe) storm per year and a 0.7% chance of a Carrington class storm per year, which can be used for planning the level of mitigation needed to protect critical national infrastructure.

1. Introduction

Extreme space weather events significantly disrupt systems for power distribution, aviation, communication, and satellites; they are driven by large-scale plasma structures emitted from the solar corona, but their impact depends on a variety of factors (Baker & Lanzerotti, 2016). Quantifying the chance of occurrence of extreme space weather events is essential to planning the resilience of vulnerable systems to catastrophic failure. Events that lead to geomagnetically induced currents that affect power grids are more likely close to solar maximum and in the descending phase of the solar cycle, but importantly, they can occur at all other times in the solar activity cycle (Thomson et al., 2010). The number of major solar eruptions varies with the approximately 11 year cycle of solar (sunspot) activity and with the amplitude of each solar cycle which is unique (Hathaway, 2015). A particular concern is the possibility of a Carrington-class event, named after the space weather superstorm of 1859 (Cliver & Dietrich, 2013; Cliver & Svalgaard, 2004; Tsurutani et al., 2003) which today could arguably cause severe disruption (Cannon et al., 2013; Daglis, 2004; Oughton et al., 2017).

Due to their rarity, amplitude and occurrence rates of space weather superstorms are challenging to quantify; it requires modeling based on the few observed large events. There have been a number of statistical studies, most of which rely on observations since the beginning of the space age. Estimates based on extrapolating a power law event distribution (Riley, 2012) suggest a 12% probability of a Carrington-class event in any given solar cycle but are highly uncertain (Riley & Love, 2016). A lognormal event distribution yields a much lower probability, again with a wide confidence interval (Love et al., 2015). Estimates based on Extreme Value Theory (Thomson et al., 2011) also suggest that the probability can be much lower (Elvidge & Angling, 2018; Siscoe, 1976; Silbergleit, 1996, 1999; Tsubouchi & Omura, 2007). More moderate storms provide a larger set of observations. When storms across different solar cycles are aggregated, there is a well-established correlation between occurrence rate and solar activity (Tsubouchi & Omura, 2007; Tsurutani et al., 2006).

©2020. The Authors.

This is an open access article under the terms of the Creative Commons Attribution License, which permits use, distribution and reproduction in any medium, provided the original work is properly cited.

Both solar wind driving (Tindale & Chapman, 2016, 2017) and geomagnetic activity (Chapman et al., 2018; Hush et al., 2015; Lockwood, Owens, et al., 2018) track the differences in the level of activity at different phases of distinct solar cycles and between cycles of different intensity.

The above statistical studies are feasible for indices which are well resolved in amplitude, such as D_{ST} . Whereas most indices, such as D_{ST} , are only available over the last five solar cycles, the aa index extends across 14 solar cycles—it is the longest almost continuous record of changes in magnetic field across the Earth's surface. Given the variability in the amplitude of different solar cycles, it is desirable to obtain event occurrence rates for this longer sample. However, the aa index is by construction based on combining observations that are logarithmically discretized in amplitude, and thus, individual records of the 3 hr aa index will have uncertainties that are both significant and nontrivial to estimate (Bubenik & Fraser-Smith, 1977).

In this Letter we propose a parameterization of extreme aa activity using averages of the annual top few percent of observed records. Our goal is to use aa to obtain a proxy for D_{ST} extremes that have occurred over the last 150 years. Our methodology is as follows. We first show that there is a good linear correlation between the annual average of the top few percent values of aa and the annual D_{ST} minimum seen over the last five solar cycles. This establishes a linear “mapping” between the annual average of the top few percentage values of aa and the annual D_{ST} minimum. We next use this linear mapping to convert these 150 annual averages of the top few percent of aa values into proxy D_{ST} extremes. This gives us 150 estimates for the annual minimum D_{ST} that occurred over the last 14 solar cycles of activity. This record then provides an estimate of how many years have included superstorm activity over the last 14 cycles, where superstorm activity is categorized in terms of the largest annual event crossing a typical threshold minimum D_{ST} level. We find that the largest samples are exponentially distributed. We can then determine the range of minimum D_{ST} that would occur if this distribution applied to the next largest record in excess of these 150 estimates, that is, a 1:151 year event. The Carrington event is also characterized in terms of its excursion in D_{ST} , and estimates vary considerably (Hayakawa et al., 2019; Siscoe et al., 2006; Tsurutani et al., 2003). We compare these estimates with the range of minimum D_{ST} for a 1:151 event inferred from the 14 solar cycle proxy D_{ST} extremes record. This provides an assessment of whether the Carrington event was a more intense version of the other superstorms that have occurred since 1868 or whether it was in a class of its own, which would require the concurrence of special conditions in the corona and solar wind and at the Earth. Only if it is the former can we use the set of observed storms to try to predict how likely such an event is in the future.

2. The Data Sets

Geomagnetic indices are derived from ground-based magnetometer observations (Mayaud, 1980) and are widely used to indicate the intensity of space weather events. The D_{ST} index (Sugiura, 1964; Sugiura & Kamei, 1991) measures low-latitude global variations in the horizontal component of the geomagnetic field, thus representing the strength of the equatorial ring current. The D_{ST} index is available (World Data Center for Geomagnetism et al., 2015) since 1957, so that we can directly compare the aa index to D_{ST} over the last five solar cycles.

We focus on the 3-hourly resolution aa index over the last 14 solar cycles, from 1868 to the present. This will be analyzed alongside the daily sunspot number which is available for the same time period. The aa index is constructed (Mayaud, 1972) from the K indices determined at two antipodal observatories (invariant magnetic latitude 50°) to provide a quantitative characterization of magnetic activity, which is homogeneous through the whole series. A key consideration for this study is that the aa index (units, nT) is discretized in amplitude (Bubenik & Fraser-Smith, 1977) since the underlying K index (Bartels et al., 1939) is a quasi-logarithmic 0–9 integer scale that characterizes the maximum positive and negative magnetic deviations that occur during each 3 hr period at a given observatory. Due to its longevity, the index has also recently required some corrections. The response seen by a magnetometer to geomagnetic activity depends on the station's location with respect to the auroral oval. A scale factor for each station is applied to the scale of threshold values used to convert the observed continuous values into quantized K values. This scale factor is adjusted for each station to allow for its location and characteristics such that the K value is a standardized measure of the level of geomagnetic activity, irrespective of the location of the observation. The Mayaud (1980) original scheme assumes that this scale factor does not change with time. This does not account for secular changes in the intrinsic geomagnetic field that have occurred over the 150 years of the aa index, which introduce a drift in the individual stations and “steps” in value as stations are changed. These

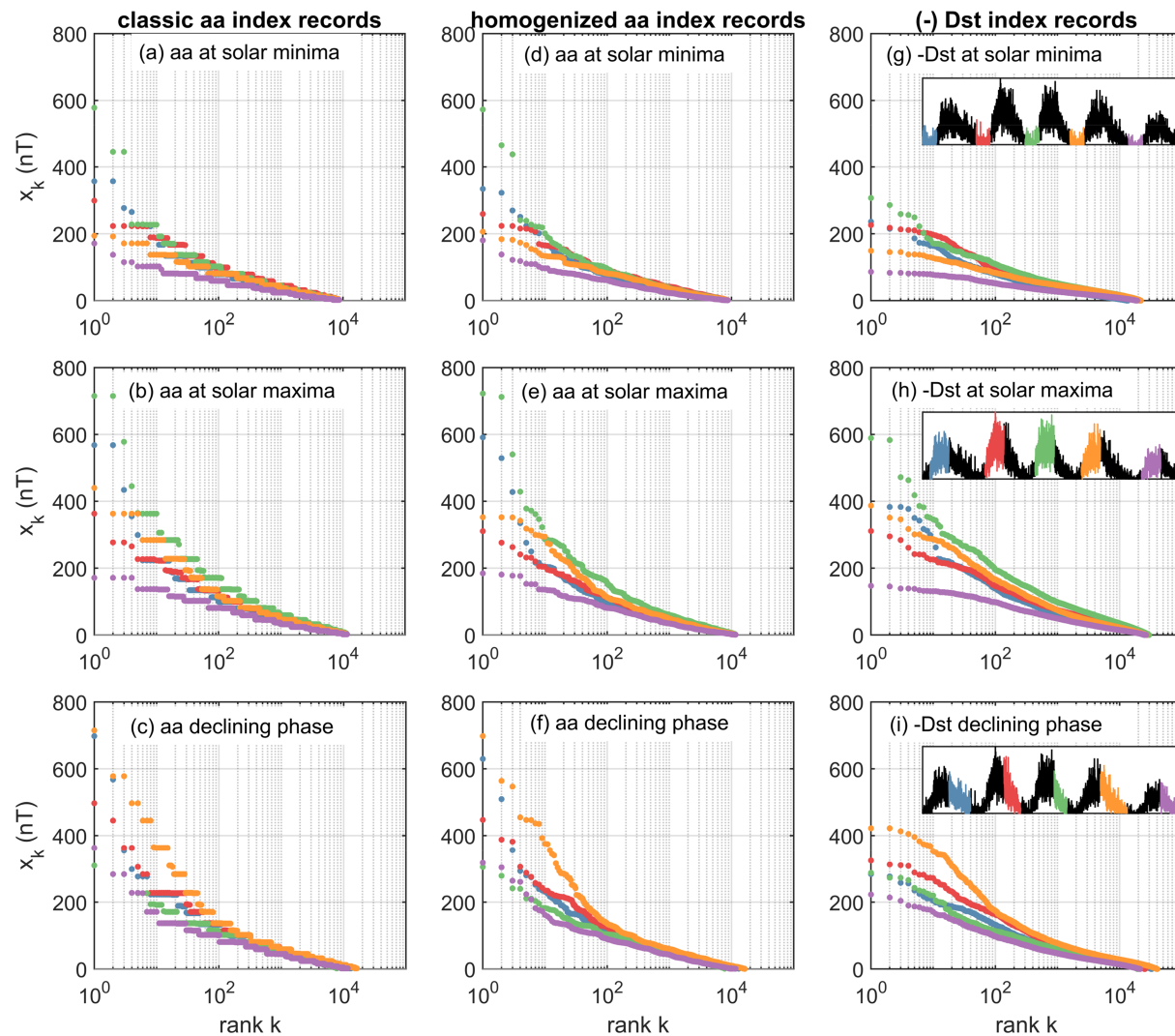


Figure 1. Rank order plots at the minima, maxima, and declining phases of the last five solar cycles plotting data records for the classic aa index (a–c), the homogenized (Lockwood, Chambodut, et al., 2018; Lockwood, Finch, et al., 2018) aa index (d–f), and $-D_{ST}$ index (g–i). The time interval from which data are used to form each rank order plot is indicated in the inset, overlapped on the daily sunspot number. Colors indicate the solar cycles 20 (blue), 21 (red), 22 (green), 23 (orange), and 24 (purple).

are discussed in detail and corrected for in Lockwood, Chambodut, et al. (2018). These corrections are typically less than 10 nT in magnitude, and while this is important for estimates of the overall long-term change in aa , it is a relatively small (and we will see, within uncertainties) perturbation on typical superstorm values. Lockwood, Finch, et al. (2018) extended this work to correct for hemispheric asymmetry using a model of the time-of-year and time-of-day response functions of the stations. They have produced a homogenized 3-hourly aa index utilizing these corrections. We have repeated the analysis here for both the homogenized and original (“classic”) versions of the aa index, and key plots that use the homogenized aa index in the main sections of the Letter are reproduced using the “classic” (ISGI) aa index in the supporting information (SI). The homogenized aa index is available to end 2017, and our analysis extends up to this date, giving 150 calendar years of data.

3. The aa Index Compared to D_{ST} at Large Values

As the aa index is nonlinearly and nonuniformly discretized in amplitude, we need to explore to what extent it can be used to characterize superstorms. We can see this by comparing it to $(-D_{ST})$, which is a well-established measure of geomagnetic storm intensity. The D_{ST} index is well sampled in amplitude, and therefore, its maximum value does provide a meaningful estimate of superstorm intensity. Semilog rank

order plots (Sornette, 2003) provide a method to display the behavior of a set of values, particularly where they are large to extreme. The observations x_k are sorted in descending amplitude and plotted (ordinate) versus their rank k (abscissa); that is, the largest observed value is Rank 1, the next largest, Rank 2, and so on. Figure 1 compares rank order plots of the data records for $(-)D_{ST}$ with that for classic and homogenized aa for the solar maximum interval, the solar minimum interval, and the declining phase of each of the last five solar cycles for which D_{ST} is available. We identify the intervals of solar minimum, solar maximum, and the declining phases by applying a single algorithm across the entire time series as detailed in the SI. In Figure 1 it is immediately apparent that the classic aa amplitude is strongly discretized at the high values, whereas $(-)D_{ST}$ resolves them. Figure 1 plots the individual data points, and the homogenized aa index shown in Figures 1d–1f) is less discretized in appearance (Lockwood, Finch, et al., 2018) than the classic aa as the individual data points have been adjusted using time- and station-dependent scale factors as discussed above. While this does correct aa for secular changes, it cannot recover the information lost by the original discretization, on a quasi-logarithmic scale, involved in constructing the K indices that underlie the aa index. Therefore, the aa maximum value (within a given interval or event) does not quantify the extrema of geomagnetic disturbances very well. As a consequence, aa is not readily amenable to standard analysis techniques for extracting and quantifying the statistical properties of events or bursts. Thus, while the Peak Over Threshold method has been successfully applied in quantifying the statistics of events in D_{ST} using Extreme Value Theory (e.g., Tsubouchi & Omura, 2007), it cannot simply be applied to the aa index. For this reason we will focus on yearlong averages of the largest 0.5% and 5% aa records seen in each year as an estimate of the relative level of extreme activity captured by the aa index. Figure 1 verifies that the large aa and $(-)D_{ST}$ records do indeed both follow the variation within and between solar cycles in the same manner despite the discretization present in the aa index. We can hence use aa to provide an indication of the variation in the extremes of geomagnetic activity over the last 14 solar cycles.

4. Historical Space Weather Activity

Figure 2 plots the level of extreme activity captured by the homogenized aa index versus annual average sunspot number from 1868–2017 inclusive, corresponding to the last 14 solar cycles. We parameterize extreme activity in aa by annual averages of the largest 0.5% (top panels) and the largest 5% (center panels) and compare this with the average of all records (bottom panels). The averages are performed over nonoverlapping calendar years. Figures 2a–2c show the parameter space explored by aa and sunspot number over the last 14 solar cycles. Figure 2c reproduces the well-known result (Feynman, 1982) that time averages of aa always exceed a baseline value which increases linearly with averaged sunspot number. A baseline can also be seen in the annual averages of the largest 0.5% and the largest 5% aa values.

We use the data from the last five solar cycles to obtain an approximate mapping between values of extreme activity in D_{ST} and aa parameterized as above. We expect from Figure 1 that the large to extreme records of aa will track those of D_{ST} . As discussed above, the amplitude of D_{ST} is well resolved, so that we can consider the single observed minimum D_{ST} record that occurs in any given calendar year as a measure of the most severe storm that occurred in that year. Figure 3 overplots versus time the nonoverlapping calendar year annual averages of the largest 0.5% of the homogenized aa index with the maximum of $(-)D_{ST}$ that occurs in the same calendar year. We see that these quantities do track each other, albeit imperfectly. Figure 2d plots (blue dots) these same quantities against each other; that is, the nonoverlapping calendar year annual averages of the largest 0.5% of the homogenized aa index are plotted versus the maximum of $(-)D_{ST}$ that occurs in each calendar year as a scatter plot. Figures 2e and 2f plot the analogous scatter plots for annual averages of the largest 5% and annual averages of aa . Since the aa index is derived from observatory K index values, it has an upper bound, whereas D_{ST} is unbounded. If the observed values of aa over the last five solar cycles (where we have contemporaneous D_{ST}) explored this upper bound, we would see a saturation or “pile up” in aa when plotted versus D_{ST} . We do not see any evidence of saturation in Figures 2d and 2e) and therefore perform a least squares linear regression fit which is plotted as the solid black line, the .95 confidence bounds are indicated by dotted lines. The r-squared coefficient of determination (which indicates the proportionate amount of variation in the response variable explained by the variable in the linear regression model) for each fit is given on the panels. Nonoverlapping calendar year annual averages of the largest 0.5% of the homogenized aa index (Figure 2d) are well described by the linear least squares fit to annual minimum D_{ST} with r-squared coefficient of determination $r = 0.81$. The coefficients of this fitted line $a(x - b)$ are (with 95% confidence intervals) $a = 0.87$, [0.76, 0.99] and $b = -43.12$ [-79.48, -6.76]. The fit is reasonable, $r = 0.76$ for

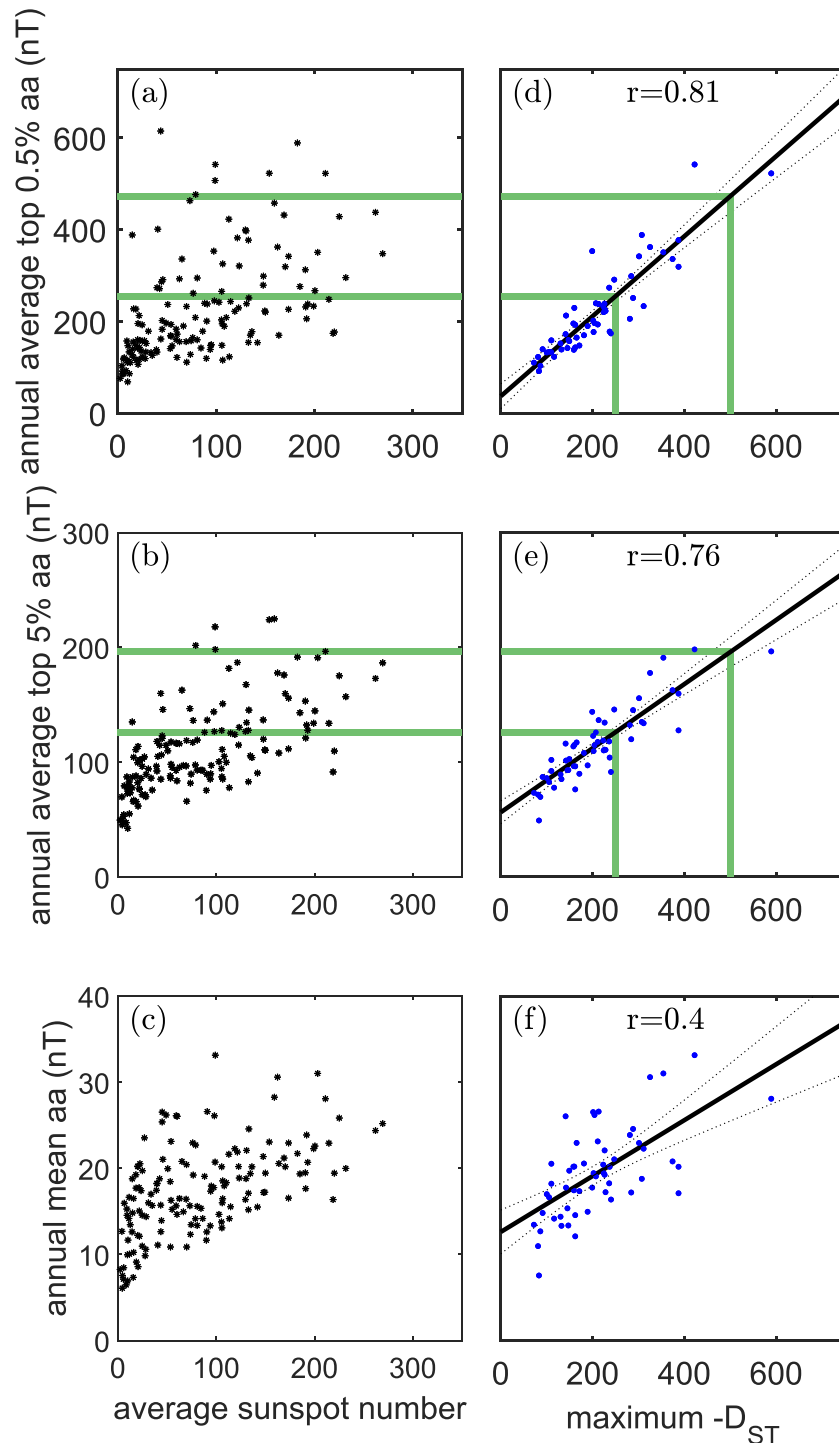


Figure 2. Panels (a–c) plot each value (black *) of the average of the largest 0.5%, largest 5%, and all homogenized *aa* index records in each calendar year, versus average sunspot number, for all observations 1868–2017 inclusive. The annual (calendar year) intervals are nonoverlapping. Panels (d–f) plot (blue dots) the subset of the nonoverlapping calendar year *aa* averages versus the maximum value of $-D_{ST}$ that occurred in the same yearlong window, taken over the last five solar cycles. In each panel the solid black line plots the least squares fit and the dotted lines, the 0.95 confidence level of the fit; the r -squared coefficient for each fit is given on the panels. The green lines use this fit to map between D_{ST} thresholds of -250 and -500 nT and corresponding *aa* values.

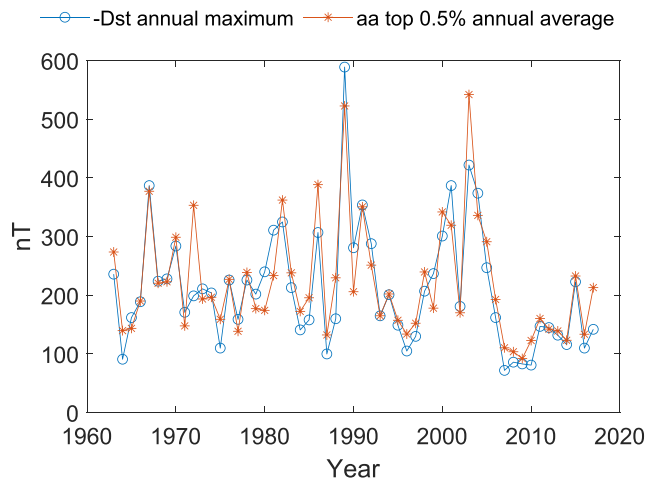


Figure 3. Comparison between $(-)D_{ST}$ and homogenized aa across the last five solar cycles. The average of the largest 0.5% homogenized aa index records in each calendar year (*) is plotted alongside the maximum $(-)D_{ST}$ (o) record that occurred in that year. The calendar year samples are nonoverlapping.

the largest 5% (Figure 2e). We need to choose a high threshold in order to isolate the largest events seen in each year of the aa index in order for these to be comparable with the largest annual minimum value of the D_{ST} index. This confirms that the correspondence is not strongly sensitive to the particular choice of high threshold. As we would expect, the correspondence will be poor between the annual averages of aa and the largest annual minimum of D_{ST} and this is indeed the case with $r = 0.4$ (Figure 2f). We therefore focus on the annual averages of the largest few percent of the aa index as the parameter for extreme activity.

We now use this least squares fit to read across between annual averages of the largest few percent of aa records to the corresponding annual D_{ST} minimum ($(-)D_{ST}$ maximum) values that would have been expected to occur over the last 14 solar cycles. Extreme space weather activity is often categorized in terms of D_{ST} crossing a minimum threshold. In Figure 2 we read across (green lines) D_{ST} levels of -250 nT, the threshold for “severe” (Riley & Love, 2016) and -500 nT, the threshold for “great” (Lakhina & Tsurutani, 2016) geomagnetic storms. D_{ST} levels of $(-250, -500)$ map onto the aa parameters as follows: annual averages of the largest 0.5% of the homogenized aa : (255, 473) and annual averages of the largest 5% of the homogenized aa (126, 196). Counting the points that lie above these thresholds in aa indicates that over 150 years, on average at least one great

storm occurred in 6 (4%) of those years, and at least one severe storm occurred in 42 (28%) of those years. These estimates average over any solar cycle variation.

We use the least squares fit in Figure 2 to read across from all 150 annual averages of the largest few percent of aa records to the corresponding D_{ST} proxy, that is, the annual D_{ST} minimum ($(-)D_{ST}$ maximum) values that would have been expected to occur over the last 14 solar cycles. These are plotted in Figure 4 as rank order plots. In addition to the 150 annual D_{ST} proxy samples, we have one additional sample that arguably exceeds all 150 values, that is, the Carrington event. The Carrington event estimate will therefore be Rank 1 on this plot. The largest of the 150 annual D_{ST} proxy samples is plotted as Rank 2, the next largest as Rank 3, and so on.

The dependencies seen on rank order plots are simply those of the distribution (Sornette, 2003) since an empirical estimate of the cumulative density function (cdf) $C(x_k)$ is obtained by plotting rank k normalized to the total number of samples, N , $C(x_k) = k/N$ versus the samples x_k arranged in ascending order of size. The leading rank observation (Rank 2 here) in 150 annual samples is then a 1/150 year event, and we indicate this and the location of a 1/10 year event across the top of the plot. To estimate the distribution functional form, we have performed a least squares fit of a straight line on this semilog plot to the 100 largest ranked D_{ST} proxy samples. The green lines plot the fitted line $x_k = \beta(\log(k) - b)$ where $k = [2..101]$ is the rank. The r-square values for these fits are high, $r > 0.99$. In Figure 4 the fit parameters with 95% confidence in brackets are $\beta = -146 [-148, -144]$ and $b = 5.53 [5.50, 5.56]$. The high r-square value of these fitted lines confirms that the tail of the distribution is well described by an exponential function (Sornette, 2003) $f(x) = (1/\beta)\exp(-x/\beta)$. The 95% confidence intervals for this fitted line give an uncertainty that deviates less than 1% from the fitted line. The dominant uncertainty on this plot arises from the variation between different empirical realizations of the cdf (or rank order plot) for which Greenwood (1926) provides an estimate as shown on the figure. Applying this uncertainty to the results from Figure 4 then gives the chance of at least one great $D_{ST} < -500$ nT storm in a given year that is then 4% with uncertainty bounds [0.9,7], and for a severe, $D_{ST} < -250$ nT storm is 28% [20,35]. The top 10 most active years in the 150 year aa record (plotted as rank $k = 2..11$ on Figure 4) are summarized in Table 1. As we would expect, years in which some of the most severe storms occurred appear here; however, we can now directly rank them and can estimate their percent occurrence likelihood.

An important question is whether the Carrington event belongs to the same physical class as the other superstorms. If so, its probable severity and chance of occurrence should be predictable at least in principle, as it will follow that of the other more moderate superstorms. If not, it is in a distinct physical class and past observations of more moderate superstorms may not inform estimates of its chance of occurrence; it

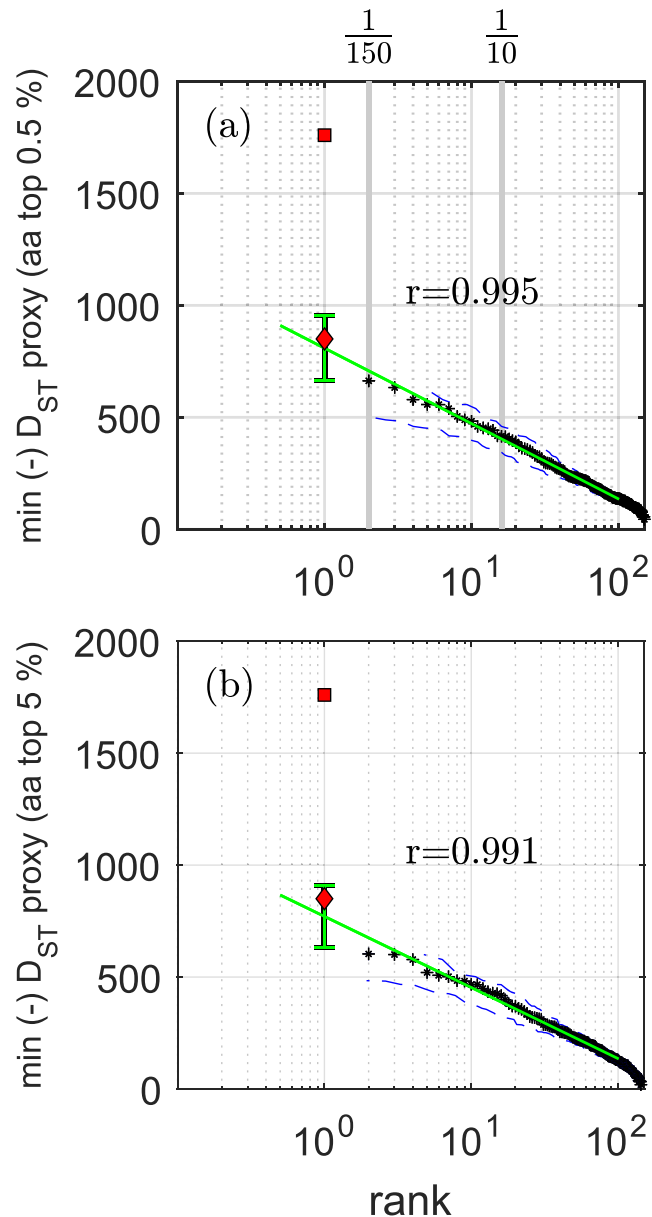


Figure 4. The panels show rank order plots of nonoverlapping annual minimum ($-$) D_{ST} proxy samples derived from (a) the largest 0.5% and (b) the largest 5% of homogenized aa (black stars). The largest of these samples is plotted as Rank 2, the next largest as Rank 3, and so on. We plot as Rank 1 two estimates of the Carrington event: $D_{ST} = -850$ nT (red diamond) and $D_{ST} = -1,760$ nT (red square). The green lines indicate an exponential fit to the largest 100 values, and the r -squared coefficient for each fit is given in the panels. The error bars for the first ranked sample (green error bar) are estimated for an underlying exponential distribution (see text). The 95% confidence level for this empirical realization of the rank order plot is estimated from Greenwood (1926) (blue dashed lines).

is a “Dragon King” (Sornette & Ouillon, 2012). We now determine if estimates for the Carrington event are consistent with the exponential distribution of proxy D_{ST} . For an exponential we have (Sornette, 2003) an estimate of the fluctuations between one realization to another for the first ranked sample, it is $\pm\beta$. This is plotted as a green error bar on Rank 1 location of the exponential fit. This gives an estimate $D_{ST} = -809$ [−663, −955] (using classic aa as shown in the SI, we obtain $D_{ST} = -813$ [−667, −959]). This is the range of values for D_{ST} for this event to be 1 in 151 year event drawn from the same distribution as other extreme activity seen in aa over the last 14 solar cycles. We overplot at Rank 1 the two estimates of the Carrington event (red diamond and square). From Figure 4 we see that the estimate of $D_{ST} = -850$ nT is consistent with the above extrapolation of the exponential fit so that the likelihood of any given year

Table 1
Rank Ordering of the Most Active Years With Chance of Occurrence from Figure 4

Top ten most active years in the <i>aa</i> index record			
Rank ^c	Year	% chance per year	Activity in that year
1	1921	0.67 [0, 1.9]	Remarkable storm ^a ; Silverman and Cliver (2001), Tables IV, VII ^b
2	1938	1.33 [0, 3.1]	Fátima storm; Tables III, IV, VII ^b
3	2003	2.0 [0, 4.2]	Halloween storms; Weaver and Murtagh (2004), Table III ^b
4	1946	2.67 [0.1, 5.2]	Table IV ^b
5	1989	3.33 [0.5, 6.3]	Quebec power outage ^a ; MacNeil (2018); Table VII ^b
6	1882	4.0 [0.9, 7.1]	Remarkable storm ^a ; Love (2018), Table IV ^b
7	1941	4.67 [1.3, 8.1]	Geomagnetic storm; Love and Coisson (2016); Tables III, IV ^b
8	1909	5.33 [1.7, 8.9]	Remarkable storm ^a ; Love et al. (2019) Tables IV, VII ^b
9	1960	6.0 [2.2, 9.8]	Table III ^b
10	1958	6.67 [2.7, 10.7]	Remarkable storm ^a ; Table VII ^b

^aRemarkable storms (geomagnetic perturbation, Table 1 of Tsurutani et al., 2003). ^bEvents in Cliver and Svalgaard (2004), Tables III (fast transit events up to 2003), IV (Greenwich list of great storms up to 1954), and VII (low-latitude auroras up to 1958). ^cRank order is derived from annual averaged top 0.5% homogenized *aa* index values plotted in Figure 4a. This need not correspond one-to-one with rankings based directly on D_{ST} for individual events.

exhibiting a Carrington-class event on this scale simply follows the exponential distribution that describes the other severe storms that have occurred since. However, a value of $D_{ST} = -1,760$ nT (red square) is in its own class of behavior; it is far from this exponential distribution tail.

The D_{ST} excursion that occurred during historical space weather events is challenging to quantify, and as a consequence, there is considerable diversity in both the values obtained and the methodology used to obtain them. The $D_{ST} = -1,760$ nT estimate for the Carrington event is a minimum magnetic displacement in a Bombay magnetogram (Tsurutani et al., 2003), and Lakhina and Tsurutani (2016) discuss supporting evidence that this is indeed consistent with this D_{ST} value. The Bombay station was fortuitously located near noon during the peak magnetometer displacement so that the effect of the disturbance field asymmetry is minimized, and local H component values are close to D_{ST} (see, e.g., Figure 2 of Siscoe et al., 2006). However, given that D_{ST} is an hourly index, this value has been interpreted by Siscoe et al. (2006) (see also Cliver & Dietrich, 2013) as a minimum $D_{ST} \approx -850$ nT based on hourly averages of the Bombay magnetogram. Different versions (Tsurutani et al., 2003; Siscoe et al., 2006) of the Burton et al. (1975) equation support these two different estimates. Other observations offer insight; Hayakawa et al. (2019) found that the equatorward boundary of auroral oval of the Carrington event was comparable with that of other superstorms, suggesting a D_{ST} value closer to that of Siscoe et al. (2006). Modeling of the “solar storm” of 2012, an intense CME which did not impact on Earth but was observed at STEREO-A, suggests extreme case scenarios of $D_{ST} = -1,182$ nT (Baker et al., 2013) and $D_{ST} = -1,150$ nT (Liu et al., 2014). In the 2012 solar storm, the correlated dynamics of several CMEs created the conditions for an unusually intense event. The analysis in this Letter does not rule out any of these estimates. Instead, it offers quantitative insight into their interpretation. Events with $D_{ST} \lesssim -1,000$ nT are a different class of behavior to other severe storms that have occurred over the last 150 years. They require special conditions which may be physical, observational, or a combination thereof.

We have parameterized extreme space weather activity with annual averages of the top few percent of the *aa* index. While this has allowed us to form a distribution from observations over 14 solar cycles, it does not discriminate the statistics of individual events. This can only be done for time series that are well resolved in amplitude, such as D_{ST} , for which there are a number of studies. We have identified a correspondence between the annual averages of the top few percent of the *aa* index and the annual minimum D_{ST} , that is, the largest event in each year. In general, for moderate conditions, there will be several storms per year, so that the return period of a level of annual activity that we find here would not be expected to correspond to the return period for an event of a specific amplitude. For the most severe and infrequent storms there will be closer correspondence between these two measures. Our estimate that a $D_{ST} \sim -850$ nT is an ~ 1 in 150 year event is not inconsistent with that of Riley and Love (2016), a 10% [1,20] chance of occurrence per decade. The D_{ST} excursion 907 ± 132 nT Love et al. (2019) estimate for the 1921 event also overlaps with the range determined here for the Rank 1 event. Tsubouchi and Omura (2007) predict an occurrence frequency

of a March 1989 storm intensity ($D_{ST} = -589$ nT) or greater as once in 60 years. In Figure 4, 1989 is ranked the fifth most active year in 150 years of aa observations, giving a return period of 30 years.

5. Conclusions

The aa index extends over the last 14 solar cycles; it is the longest almost continuous record of geomagnetic activity at the Earth's surface. However, the aa index is constructed from observations that are logarithmically discretized in amplitude and thus individual records of the 3 hr aa index will have uncertainties that are both significant and nontrivial to estimate (Bubenik & Fraser-Smith, 1977); in particular, its extreme excursions are not well resolved in amplitude. We parameterized extreme aa activity using averages of the annual top few percent of observed records. Our analysis based on rank order plots (Sornette, 2003) shows that the distribution tail (of the top 100 annual estimates of extreme aa activity) is well described by an exponential distribution ($r > 0.99$). The D_{ST} index is available for the last five solar cycles, and as its amplitude is well resolved it is commonly used to characterize the intensity of space weather events. We found a good correspondence ($r \sim 0.8$) between the annual minimum D_{ST} value and the annual-averaged top few (0.5%, 5%) values of aa over the last five solar cycles. This can be used to “read across” between annual minimum D_{ST} values and extreme activity in aa .

We then find that least one “severe” storm of $D_{ST} < -250$ nT occurred in each of 42 (~28% [20,35]) of those years, and at least one “great” storm $D_{ST} < -500$ nT occurred in each of 6 (~4% [0.9,7]) of those years. These estimates are an overall average and do not take into account any solar cycle phase variation. By sampling over 14 solar cycles, they do include a greater variety of solar cycle intensities than estimates that rely upon data from the last five cycles.

We extended this analysis to D_{ST} estimates for the Carrington event, to compare them with the annual level of extreme activity seen in aa . Extrapolating our exponential distribution gives an estimate $D_{ST} = -809$ [−663, −955] for a 1 in 151 year event that follows the same distribution as other extreme activity seen in aa over the last 14 solar cycles. The occurrence of a $D_{ST} \sim -850$ nT (Siscoe et al., 2006) event in a single year is consistent with this distribution tail. A Carrington event on this scale is a more intense version of the other superstorms that have occurred since 1868, so that in this case the set of observed superstorms can be used to predict how likely such an event is in the future. A $D_{ST} \sim -1,760$ nT Carrington event on the other hand is far from the distribution tail and is in a class of its own, it is a “Dragon King” (Sornette & Ouillon, 2012) requiring the concurrence of special conditions in the corona and solar wind and at the Earth. The 2012 “solar storm” (Liu et al., 2014) is an event in this class, where the correlated dynamics of several CMEs created the conditions for an unusually intense event.

References

Baker, D. N., & Lanzerotti, L. J. (2016). Resource letter SW1: Space weather. *American Journal of Physics*, *84*, 166. <https://doi.org/10.1119/1.4938403>

Baker, D. N., Li, X., Pulkkinen, A., Ngwira, C. M., Mays, M. L., Galvin, A. B., & Simunac, K. D. C. (2013). A major solar eruptive event in July 2012: Defining extreme space weather scenarios. *Space Weather*, *11*, 585. <https://doi.org/10.1002/swe.20097>

Bartels, J., Heck, N. H., & Johnston, H. F. (1939). *The three-hour-range index measuring geomagnetic activity* (Vol. 44, pp. 411–454). <https://doi.org/10.1029/TE044i004p00411>

Bubenik, D. M., & Fraser-Smith, A. C. (1977). Evidence for strong artificial components in the equivalent linear amplitude geomagnetic indices. *Journal of Geophysical Research*, *82*, 2875.

Burton, R. K., McPherron, R. L., & Russell, C. (1975). An empirical relationship between interplanetary conditions and *Dst*. *Journal of Geophysical Research*, *80*, 4204.

Cannon, P., Angling, M., Barclay, L., Curry, C., Dyer, C., Edwards, R., et al. (2013). Extreme space weather: Impacts on engineered systems and infrastructure. In *Royal Academy of Engineering*, London, United Kingdom, pp. 1–68.

Chapman, S. C., Watkins, N. W., & Tindale, E. (2018). Reproducible aspects of the climate of space weather over the last five solar cycles. *Space Weather*, *16*, 1128–1142. <https://doi.org/10.1029/2018SW001884>

Cliver, E. W., & Dietrich, W. F. (2013). The 1859 space weather event revisited: Limits of extreme activity. *Journal of Space Weather and Space Climate*, *3*, 31. <https://doi.org/10.1051/swsc/2013053>

Cliver, E. W., & Svalgaard, L. (2004). The 1859 solar-terrestrial disturbance and the current limits of extreme space weather activity. *Solar Physics*, *224*, 407–422.

Daglis, I. A. (Ed.). (2004). *Effects of space weather on technology infrastructure* (pp. 1–334). Dordrecht The Netherlands: Kluwer Academic Publishers.

Elvidge, S., & Angling, M. J. (2018). *Using extreme value theory for determining the probability of Carrington-like solar flares* (Vol. 16, pp. 417–421). <https://doi.org/10.1002/2017SW001727>

Feynman, J. (1982). Geomagnetic and solar wind cycles, 1900–1975. *Journal of Geophysical Research*, *87*(A8), 6153. <https://doi.org/10.1029/JA087iA08p06153>

Acknowledgments

The results presented in this paper rely in part on geomagnetic indices calculated and made available by ISGI Collaborating Institutes from data collected at magnetic observatories. We acknowledge the involved national institutes, the INTERMAGNET network, and ISGI (isgi.unistra.fr). We also acknowledge Lockwood, Chambodut, et al. (2018) and Lockwood, Finch, et al. (2018) for the provision of the homogenous aa index used here. We thank the World Data Center for Geomagnetism, Kyoto. We thank the World Data Center SILSO, Royal Observatory of Belgium, Brussels, for provision of sunspot data. S. C. C. acknowledges a Fulbright-Lloyd's of London Scholarship and AFOSR Grants FA9550-17-1-0054 and ST/P000320/1. R. B. H. acknowledges the NERC Highlight topic Grants NE/P01738X/1 (Rad-Sat) and NE/R016038/1. Data availability: The ISGI aa index data set analyzed here was downloaded from the International Service of Geomagnetic Indices (<http://isgi.unistra.fr/>). The homogenized aa index analyzed here was downloaded from the SI of Lockwood, Finch, et al. (2018) (<https://www.swsc-journal.org/articles/swsc/olm/2018/01/swsc180022/swsc180022.html>). The daily sunspot number data set was downloaded from the SILSO, World Data Center-Sunspot Number and Long-term Solar Observations, Royal Observatory of Belgium, online Sunspot catalog (<http://www.sidc.be/SILSO/>), “1868–2017”. The D_{ST} index analyzed here was downloaded from NASA/GSFC's Space Physics Data Facility's OMNIWeb service; the OMNI data were obtained from the GSFC/SPDF OMNIWeb interface (<https://omniweb.gsfc.nasa.gov>).

- Greenwood, M. (1926). *The natural duration of cancer, in reports of public health and related subjects* (Vol. 33). London: HMSO.
- Hathaway, D. H. (2015). The solar cycle. *Living Reviews in Solar Physics*, 12, 4. <https://doi.org/10.1007/lrsp-2015-4>
- Hayakawa, H., Ebihara, Y., Willis, D. M., Toriumi, S., Iju, T., Hattori, K., et al. (2019). Temporal and spatial evolutions of a large sunspot group and great auroral storms around the Carrington event in 1859. *Space Weather*, 17, 1553–1569. <https://doi.org/10.1029/2019SW002269>
- Hush, P., Chapman, S. C., Dunlop, M. W., & Watkins, N. W. (2015). Robust statistical properties of the size of large burst events in *AE*. *Geophys Research Letters*, 42, 9197–9202. <https://doi.org/10.1002/2015GL066277>
- Lakhina, G. S., & Tsurutani, B. T. (2016). Geomagnetic storms: Historical perspective to modern view. *Geoscience Letters*, 3, 5. <https://doi.org/10.1186/s40562-016-0037-4>
- Liu, Y. D., Luhmann, J. G., Kajdic, P. E., Kilpua, K. J., Lugaz, N., Nitta, N. V., et al. (2014). Observations of an extreme storm in interplanetary space caused by successive coronal mass ejections. *Nature Communications*, 5, 3481. <https://doi.org/10.1038/ncomms4481>
- Lockwood, M., Chambodut, A., Barnard, L. A., Owens, M. J., & Clarke, E. (2018). A homogeneous *aa* index: 1. Secular variation. *Journal Space Weather and Space Climate*, 8(A53). <https://doi.org/10.1051/swsc/2018038>
- Lockwood, M., Finch, I. D., Chambodut, A., Barnard, L. A., Owens, M. J., & Clarke, E. (2018). A homogeneous *aa* index: 2. Hemispheric asymmetries and the equinoctial variation. *Journal Space Weather Space Climate*, 8(A58).
- Lockwood, M., Owens, M. J., Barnard, L. A., Scott, C. J., Watt, C. E., & Bentley, S. (2018). Space climate and space weather over the past 400 years: 2. Proxy indicators of geomagnetic storm and substorm occurrence. *Journal Space Weather Space Climate*, 8(A12), 19. <https://doi.org/10.1051/swsc/2017048>
- Love, J. J. (2018). The electric storm of November 1882. *Space Weather*, 16, 37–46. <https://doi.org/10.1002/2017SW001795>
- Love, J. J., & Coisson, P. (2016). The geomagnetic blitz of September 1941. *Eos*, 97. <https://doi.org/10.1029/2016EO059319>
- Love, J. J., Hayakawa, H., & Cliver, E. W. (2019). On the intensity of the magnetic superstorm of September 1909. *Space Weather*, 17, 37–45. <https://doi.org/10.1029/2018SW002079>
- Love, J. J., Hayakawa, H., & Cliver, E. W. (2019). Intensity and impact of the New York Railroad superstorm of May 1921. *Space Weather*, 17, 1281–1292. <https://doi.org/10.1029/2019SW002250>
- Love, J. J., Rigler, E. J., Pulkkinen, A., & Riley, P. (2015). On the lognormality of historical magnetic storm intensity statistics: Implications for extreme-event probabilities. *Geophysical Research Letters*, 42, 6544–6553. <https://doi.org/10.1002/2015GL064842>
- MacNeil, J. (2018). Solar explosion leads to blackout, March 10, 1989 EDN Network March 10.
- Mayaud, P.-N. (1972). The *aa* indices: A 100 year series characterizing the magnetic activity. *Journal of Geophysical Research*, 77, 6870.
- Mayaud, P. N. (1980). *Derivation, meaning, and use of geomagnetic indices*. *Geophys. Monogr. Ser.* (Vol. 22). Washington DC: AGU. <https://doi.org/10.1029/GM022>
- Oughton, E. J., Skelton, A., Horne, R. B., Thomson, A. W. P., & Gaunt, C. T. (2017). Quantifying the daily economic impact of extreme space weather due to failure in electricity transmission infrastructure. *Space Weather*, 15, 65–83. <https://doi.org/10.1002/2016SW001491>
- Riley, P. (2012). On the probability of occurrence of extreme space weather events. *Space Weather*, 10, S02012. <https://doi.org/10.1029/2011SW000734>
- Riley, P., & Love, J. J. (2016). Extreme geomagnetic storms: Probabilistic forecasts and their uncertainties. *Space Weather*, 15, 53–64. <https://doi.org/10.1002/2016SW001470>
- Silbergleit, V. M. (1996). On the occurrence of geomagnetic storms with sudden commencements. *Journal of Geomagnetism and Geoelectricity*, 48, 1011.
- Silbergleit, V. M. (1999). Forecast of the most geomagnetically disturbed days. *Earth, Planets and Space*, 51, 19. <https://doi.org/10.1186/BF03352205>
- Silverman, S. M., & Cliver, E. W. (2001). Low-latitude auroras: The magnetic storm of 14-15 May 1921. *Journal of Atmospheric and Solar Terrestrial Physics*, 63(5), 523–535.
- Siscoe, G. L. (1976). On the statistics of the largest geomagnetic storms per solar cycle. *Journal of Geophysical Research*, 81, 4782. <https://doi.org/10.1029/JA081i025p04782>
- Siscoe, G., Crooker, N. U., & Clauer, C. R. (2006). D_{st} of the Carrington storm of 1859. *Advances in Space Research*, 38, 173–179.
- Sornette, D. (2003). *Critical phenomena in natural sciences* (2nd ed.). Berlin: Springer.
- Sornette, D., & Ouillon, G. (2012). Dragon-kings: Mechanisms, statistical methods and empirical evidence. *The European Physical Journal Special Topics* 205, 1, 1–26.
- Sugiura, M. (1964). Hourly value of equatorial Dst for the IGY. *Ann. Int. Geophys. Year*, 35, 9–45.
- Sugiura, M., & Kamei, T. (1991). Equatorial Dst index 1957–1986. In *AGA Bull.*, 40 ISGI Publication Office, Saint-Maur-des-Fosses, France.
- Thomson, A. W. P., Dawson, E. B., & Reay, S. J. (2011). Quantifying extreme behaviour in geomagnetic activity. *Space Weather*, 9, S10001. <https://doi.org/10.1029/2011SW000696>
- Thomson, A. W. P., Gaunt, C. T., Cilliers, P., Wild, J. A., Opperman, B., McKinnell, L.-A., et al. (2010). Present day challenges in understanding the geomagnetic hazard to national power grids. *Advances in Space Research*, 45, 1182–1190. <https://doi.org/10.1016/j.asr.2009.11.023>
- Tindale, E., & Chapman, S. C. (2016). Solar cycle variation of the statistical distribution of the solar wind ϵ parameter and its constituent variables. *Geophysical Research Letters*, 43, 5563–5570. <https://doi.org/10.1002/2016GL068920>
- Tindale, E., & Chapman, S. C. (2017). Solar wind plasma parameter variability across solar cycles 23 and 24: From turbulence to extremes. *Journal of Geophysical Research: Space Physics*, 122, 9824–9840. <https://doi.org/10.1002/2017JA024412>
- Tsubouchi, K., & Omura, Y. (2007). Long-term occurrence probabilities of intense geomagnetic storm events. *Space Weather*, 5, S12003. <https://doi.org/10.1029/2007SW000329>
- Tsurutani, B. T., Gonzalez, W. D., Lakhina, G. S., & Alex, S. (2003). The extreme magnetic storm of 1-2 September 1859. *Journal of Geophysical Research*, 108(A7), 1268. <https://doi.org/10.1029/2002JA009504>
- Tsurutani, B. T., Gonzalez, W. D., Lakhina, G. S., & Alex, S. (2006). Corotating solar wind streams and recurrent geomagnetic activity: A review. *Journal of Geophysical Research*, 111, A07S01. <https://doi.org/10.1029/2005JA011273>
- Weaver, M., & Murtagh, W. (Eds.) (2004). Halloween space weather storms of 2003 (NOAA Technical Memorandum OAR SEC-88). Boulder CO: Space Environment Center. OCLC, 68692085.
- World Data Center for Geomagnetism, Nose, K. M., Iyemori, T., Sugiura, M., & Kamei, T. (2015). Geomagnetic Dst index. <https://doi.org/10.17593/14515-74000>